



OPEN ACCESS

EDITED BY

Hans Von Storch,
Helmholtz Zentrum Hereon, Germany

REVIEWED BY

Jinfang Yin,
Chinese Academy of Meteorological
Sciences, China
Huopo Chen,
Institute of Atmospheric Physics (CAS),
China

*CORRESPONDENCE

Noriko N. Ishizaki,
✉ ishizaki.noriko@nies.go.jp

SPECIALTY SECTION

This article was submitted to
Atmospheric Science,
a section of the journal
Frontiers in Earth Science

RECEIVED 22 November 2022

ACCEPTED 28 February 2023

PUBLISHED 21 March 2023

CITATION

Ishizaki NN, Nakaegawa T, Pinzón R and
Sasaki H (2023), Factors contributing to
morning rain in the upper Río Chagres
Basin, Panamá.
Front. Earth Sci. 11:1105013.
doi: 10.3389/feart.2023.1105013

COPYRIGHT

© 2023 Ishizaki, Nakaegawa, Pinzón and
Sasaki. This is an open-access article
distributed under the terms of the
[Creative Commons Attribution License
\(CC BY\)](#). The use, distribution or
reproduction in other forums is
permitted, provided the original author(s)
and the copyright owner(s) are credited
and that the original publication in this
journal is cited, in accordance with
accepted academic practice. No use,
distribution or reproduction is permitted
which does not comply with these terms.

Factors contributing to morning rain in the upper Río Chagres Basin, Panamá

Noriko N. Ishizaki^{1*}, Tosiya Nakaegawa², Reinhardt Pinzón³ and Hidetaka Sasaki¹

¹Center for Climate Change Adaptation, National Institute for Environmental Studies, Tsukuba, Ibaraki, Japan, ²Department of Applied Meteorology Research, Meteorological Research Institute, Tsukuba, Ibaraki, Japan, ³Universidad Tecnológica de Panamá, Centro de Investigaciones Hidráulicas e Hidrotécnicas, Group HPC-Cluster-Iberogun, Panamá City, Panamá

The Upper Chagres River Basin plays an important role in the stable operation of the Panama Canal. Previous studies have shown that there is a salient regional difference in the diurnal variation of precipitation in the basin. Precipitation during the rainy season peaks in the early afternoon throughout the basin, but precipitation is also observed in the morning at sites in the northern part of the basin. However, the cause of this is not clear due to limited ground observation. To address this issue, we conducted dynamical downscaling experiments with a horizontal grid spacing of 5 and 2 km and nested in a global atmospheric model with horizontal grid spacing of approximately 20 km. The results showed that the 2 km convection-permitting model successfully reproduced regional differences in observed diurnal variations. The downscaled results indicated that intensified low-level northeasterly winds over the southern Caribbean Sea triggered favorable conditions for morning rain with an orographic effect under the seaside coastal regime in the western Caribbean Sea. This is in contrast to precipitation peaks in the early afternoon under a landside coastal regime.

KEYWORDS

precipitation, Panama, diurnal cycle, morning rain, regional climate model

1 Introduction

The climate in the tropics is characterized by strong diurnal variations of precipitation. A diurnal change in precipitation is the main driver of various daily variations in the hydrologic cycle, and it is important to investigate these regional characteristics and underlying physical mechanisms. Therefore, many studies have been conducted on this topic (e.g., [Yang and Slingo \(2001\)](#); [Ohsawa et al., 2001](#); [Kikuchi and Wang, 2008](#)). For example, [Mori et al. \(2004\)](#) analyzed the diurnal cycle of precipitation over Sumatra Island and the Indonesian maritime continents using the Tropical Rainfall Measuring Mission (TRMM) satellite and rawinsonde sounding data. This study showed that convective precipitation with a peak occurred in the late afternoon over the land regions of Sumatra Island, whereas rainfall occurred in the early morning over the surrounding sea region. They also found that a precipitation peak emerges near the coast in the early morning and then migrates offshore. This feature around Indonesia is confirmed by a number of papers (e.g., [Fujita et al., 2013](#)) and in other tropical coastal areas (e.g., [Houze et al., 1981](#); [Mapes et al., 2003](#); [Ichikawa and Yasunari, 2008](#)).

The Panamanian climate also shows a strong diurnal variation. Panama is located between the Caribbean Sea and the Pacific Ocean, and its climate is influenced by various large-scale phenomena such as the El Niño-Southern Oscillation (ENSO) and tropical lower

jet. Wet and dry seasons are observed as the Inter-Tropical Convergence Zone (ITCZ) shifts (e.g., Nakaegawa et al., 2014a; 2015). In the vicinity of Panama, diurnal cycles have been mainly analyzed based on satellites and numerical simulations. Sorooshian et al. (2002) investigated daily changes in tropical precipitation intensity using precipitation estimation from remote sensing information and an artificial neural network system. They showed that strong convective precipitation predominates from morning to late afternoon south of the Isthmus of Panama in the summer, whereas there is a peak in the morning over the waters north of Panama. Over land, the convective cycle is concentrated between 14–18 local time (LT). Mapes et al. (2003) showed differences in the daily summer precipitation cycle between land and the Caribbean and Pacific coasts, which were generally reproduced in the short-term integrated results using a regional model (Warner et al., 2003). In Costa Rica, an analysis of TRMM showed that convective activity peaks in the afternoon in many areas, except along the Caribbean coast (Rapp et al., 2014).

On one hand, precipitation over land tends to have a maxima in the late afternoon and early evening, whereas precipitation over the open ocean tends to be maximal in the early morning. On the other hand, the diurnal cycle is known to be complicated in coastal areas (Xie et al., 2006; Biasutti et al., 2012). Kikuchi and Wang (2008) identified three regimes of global tropical diurnal precipitation according to the amplitude, peak time, and phase propagation characteristics of diurnal precipitation. According to their analysis, Panama is categorized as part of the landside coastal regime with landward phase propagation and peaks occurring from noon to evening. As shown in the analysis using satellite-based observations and numerical simulations, Nakaegawa et al. (2019) revealed that the diurnal cycle of precipitation at four rain gauges located in the Upper Chagres River Basin peaks in the early afternoon. However, they also showed that there are salient regional differences in the diurnal cycle even over land. They demonstrated that Chamon and Esperanza, which are located in the northern part of the Upper Chagres River Basin, have morning rain and afternoon

precipitation peaks. However, the factors that are responsible for this have not been clarified. According to the ground observation data utilized by Nakaegawa et al. (2019), the morning rain (00–12 LT) in August accounts for 45%–50% of the daily precipitation at stations in the northern part of the Upper Chagres River Basin. Therefore, it is very important to investigate the factors responsible for regional differences in the diurnal cycle of precipitation to consider the stable operation of the Panama Canal.

In this study, we identify the regional characteristics of diurnal changes in precipitation in Panama and the factors that contribute to these differences. For this purpose, we analyze the results of dynamical downscaling products using a regional model for the vicinity of Panama.

2 Data and model

In this study, 5-km and 2-km grid spacing non-hydrostatic regional climate model systems (NHRCM; Sasaki et al., 2011; Ishizaki et al., 2012) were used (Figure 1). NHRCM was developed based on the operational forecast model, which is intended for simulation of the long-term climate (Sasaki et al., 2011). The Kain–Fritsch convective parameterization scheme (Kain and Fritsch, 1993) was used for the NHRCM with 5-km grid spacing (NHRCM05), while the NHRCM with 2-km grid spacing (NHRCM02) was employed as a convection-permitting model. The cloud microphysical scheme used in NHRCM consists of cloud ice, snow, and graupel (Ikawa and Saito, 1991) based on Lin et al. (1983). Further details can be found in Saito et al. (2001). The MRI-JMA Simple Biosphere scheme (MJ-SiB) was implemented to simulate the land surface hydrological process, land surface temperature, and snow depth (Hirai et al., 2007) and is suitable for long-term simulations. A 20-year time-slice experiment (from 1980 to 2000) was conducted using the one-way nesting method. Experiments were conducted for 13-month periods every year starting on December 1, while the first month was

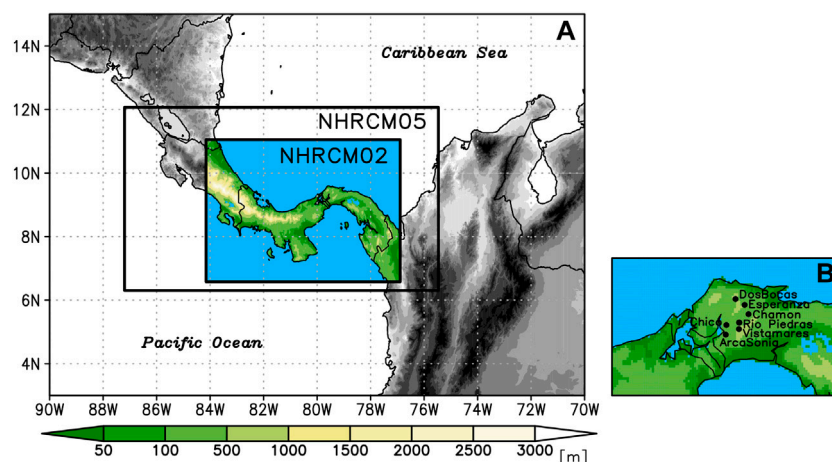


FIGURE 1

Calculation domains for NHRCM05/02 (A) and locations of rain gauge stations (B). The colors indicate elevation.

TABLE 1 List of rain gauge stations and data periods used in this study. The location column shows whether the area is located north or south of 9.3°N.

Station name	Abbreviation	Location	Period
Esperanza	EZA	North	1998–2016
Dos Bocas	DBK	North	2000–2016
Chamon	CHM	North	2000–2016
Chico	CHI	South	1967–2016
Rio Piedras	RPAC	South	1985–2016
Arca Sonia	ARC	South	1999–2016
Vistamares	VTM	South	1998–2016

excluded as a spin-up period. We first employed NHRCM05, which was driven by a 20-km grid spacing atmospheric general circulation model (MRI-AGCM3.2; Mizuta et al., 2006), and then, NHRCM02 was nested into NHRCM05. This type of modeling system and experimental setups have already been applied to the Philippines (Cruz et al., 2016), Vietnam (Kieu-Thi et al., 2016), Thailand (Takayabu et al., 2021), and Japan (e.g., Kawase et al., 2020). The fundamental evaluation of model performances is described in Pinzón et al. (2021). A comparison with the satellite-based observation revealed good performance of NHRCM in representing the seasonal variation of surface air temperature and precipitation.

Three-dimensional outputs of the MRI-AGCM3.2 with 12 vertical layers were also used in the analysis. It is important to note that the horizontal grid spacing of the data was aggregated to 1.25-degree and the temporal interval was 6 h. The atmospheric data on the pressure level were also utilized from the Japanese 55-year Reanalysis or JRA-55 (Kobayashi et al., 2015).

Hourly precipitation data at seven rain gauge stations (Table 1; Nakaegawa et al., 2019) were utilized as observations. The dynamical downscaling domain and gauge stations are shown in Figure 1.

3 Results

To confirm whether the NHRCMs reproduce the diurnal variation in precipitation at observation stations in each month, we compared simulated precipitation at the nearest grid with an observation (Figure 2). At Dos Bocas (DBK) and Esperanza (EZA) in the northern part of the basin, significant precipitation is observed from April to December, with a precipitation peak around 14 local time (LT) in May to October. As demonstrated by Nakaegawa et al. (2019), precipitation also occurred in the morning, especially in the early rainy season. Similar precipitation patterns were also observed in Chamon (CHM), while in Rio Piedras (RPAC), Vistamares (VTM), Chico (CHI), and Arca Sonia (ARC), which are located in the southern part of the basin, precipitation peaks occurred around 14 LT and morning rain was rarely observed. NHRCM05 overestimated both the magnitude and duration of afternoon precipitation, which is considered the main cause of total precipitation overestimation, and a precipitation peak was slightly later than that observed. Precipitation was also

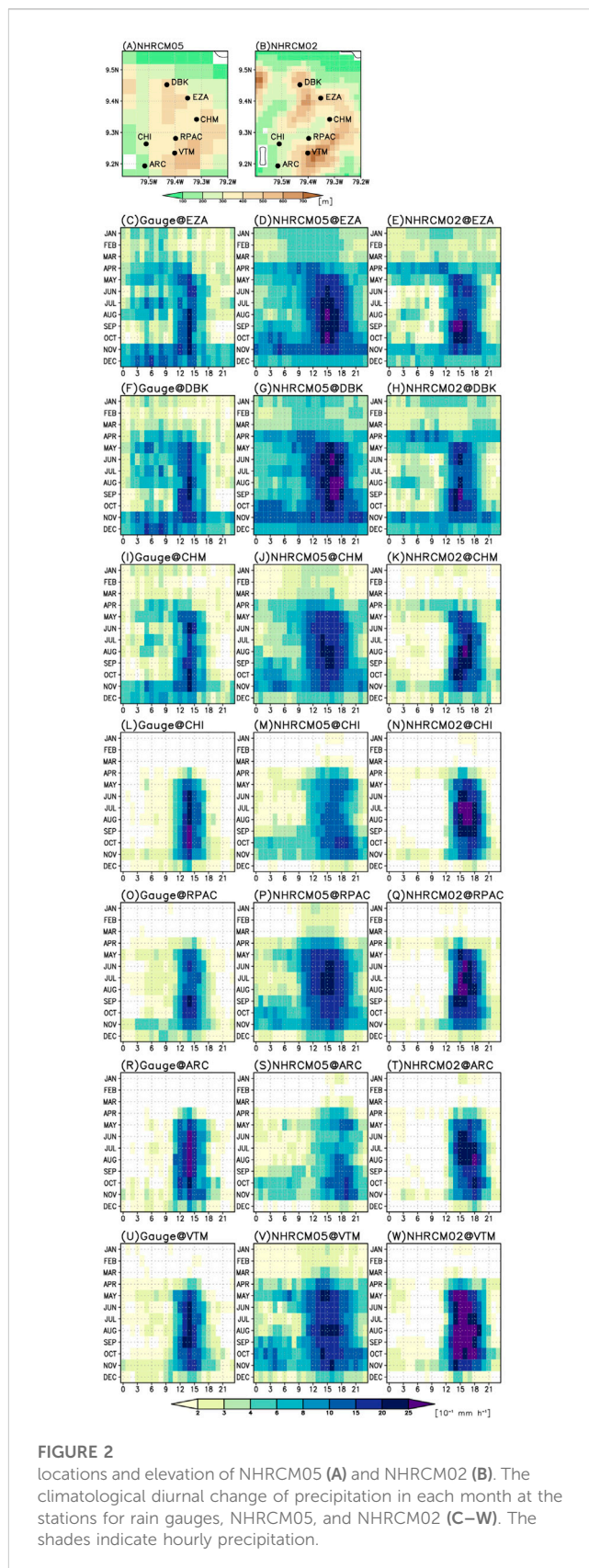
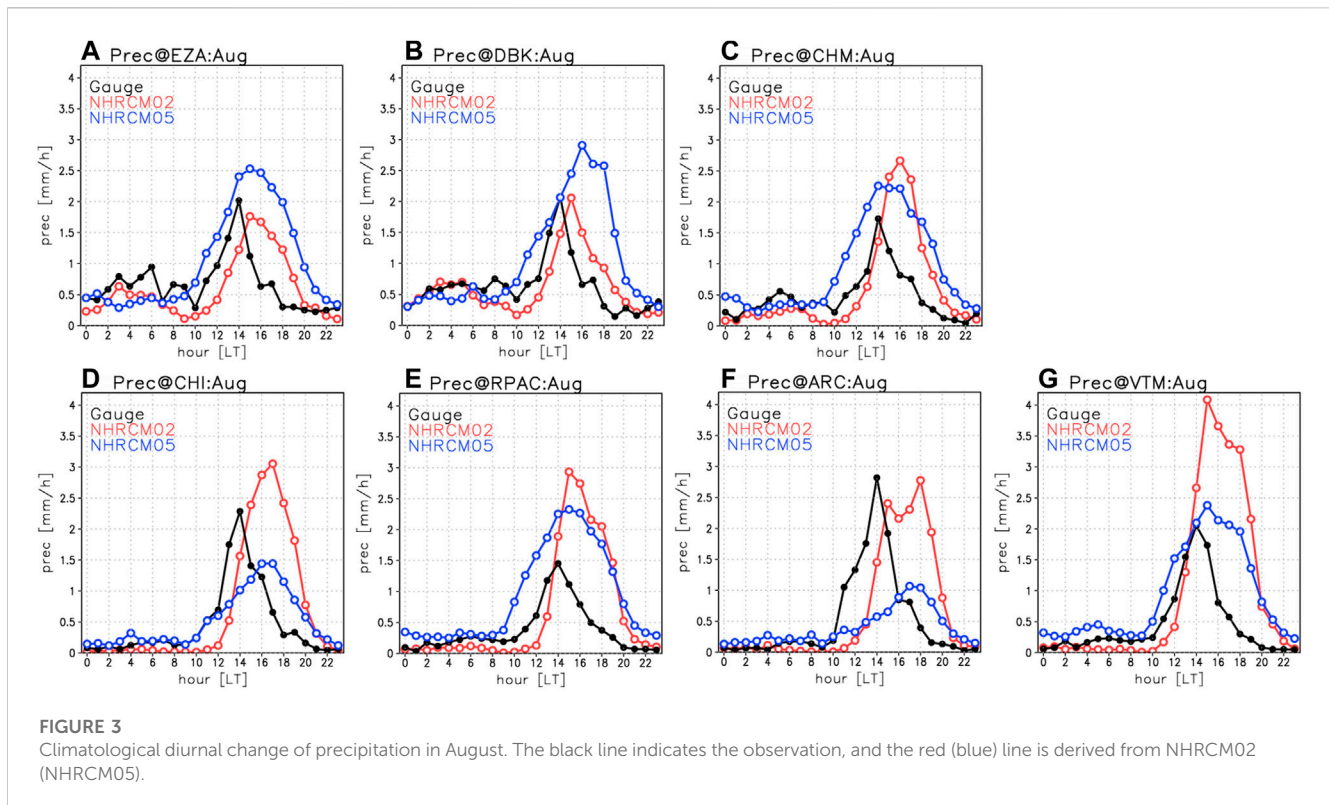


FIGURE 2 locations and elevation of NHRCM05 (A) and NHRCM02 (B). The climatological diurnal change of precipitation in each month at the stations for rain gauges, NHRCM05, and NHRCM02 (C–W). The shades indicate hourly precipitation.

represented in the morning during the rainy season at DBK, EZA, and CHM, but the amount of precipitation was relatively low compared to the afternoon peak. Furthermore, morning rain



was found in NHRCM05 even in the southern part of the basin where morning rain is rarely observed. Morning rains were clearly shown in the beginning (April) and end (November) of the rainy season in NHRCM05, which is different from the observed feature. NHRCM02 showed a shorter duration of afternoon precipitation than NHRCM05 (Figure 2). Precipitation peaks occurred about one or two hours later than observed in many stations, but precipitation amounts were comparable to those observed, except in the southern part of the basin. Furthermore, morning rain observed in the northern part of the basin during the first half of the rainy season was also well reproduced. Figure 3 shows the diurnal variation in precipitation in August. As described previously, NHRCM05 has prolonged afternoon precipitation, which results in an excess of total precipitation. The peak time of precipitation is delayed by an hour or two from that observed at many stations, and the beginning of precipitation is also earlier. However, NHRCM02 generally reproduces good precipitation duration and peak precipitation amounts in the northern part of the basin. In the southern part of the basin, peak precipitation is more excessive than in NHRCM05. Although the amount of precipitation was larger than the observation, the diurnal change and regional differences were represented in NHRCM05 and NHRCM02. This indicates that the factors that bring local morning rain over land may also be reproduced in the numerical model.

We analyzed the atmospheric features in days when local morning rain occurred in the northern part of the headland of Panama (domain A in Figure 4; 79.2–79.7°W, 9.4–9.6°N). This area belongs to the province of Colon. We constructed the much morning rain-day composite (MRcomp) as defined when the precipitation in domain A for 07–12 LT exceeds 1 mm, while the

not much morning-rain-day composite (NRcomp) consists of days with morning rain less than 0.1 mm. The sample sizes of MRcomp and NRcomp in August were 81 and 284 days, respectively. Figure 4 shows the characteristics of composited precipitation and surface wind at different times of the day for MRcomp and NRcomp. In the late afternoon prior to the occurrence of morning rain, there is less precipitation over land in MRcomp than in NRcomp (Figures 4B,C). The northeasterly winds from the Caribbean Sea are remarkably stronger in MRcomp. Compared with NRcomp, precipitation in MRcomp was larger over the Caribbean Sea, whereas it was less over the Pacific Ocean. In the early morning, the surface winds over the Caribbean Sea are enhanced in MRcomp, which is associated with an intense northeasterly over the eastern Caribbean Sea along the coast (Figures 4D,E). The precipitation area with a peak over the coastal region extends over land in the northern headland of Panama. Precipitation tends to be high off the Gulf of Panama coast during morning rain events. The coastal precipitation over the Caribbean Sea was relatively high even in 07–12 LT (Figure 4G). Strong northeasterly winds continued until evening (Figure 4I). The precipitation mainly occurs over land at this time, and the precipitation pattern was similar between MRcomp and NRcomp. The long-lasting and strong northeasterly winds over the Caribbean Sea characterize the MRcomp.

To examine wind changes in the surrounding region, 2-day composites were created prior to the morning rain event. We detected the day if the morning rain in domain A of the day exceeded 1 mm and the morning rain of the day before did not exceed 1 mm. The sample size was 59 cases. The longitude-time cross sections are shown in Figure 5. From a climatological view, easterly winds are predominant and have a pronounced daily

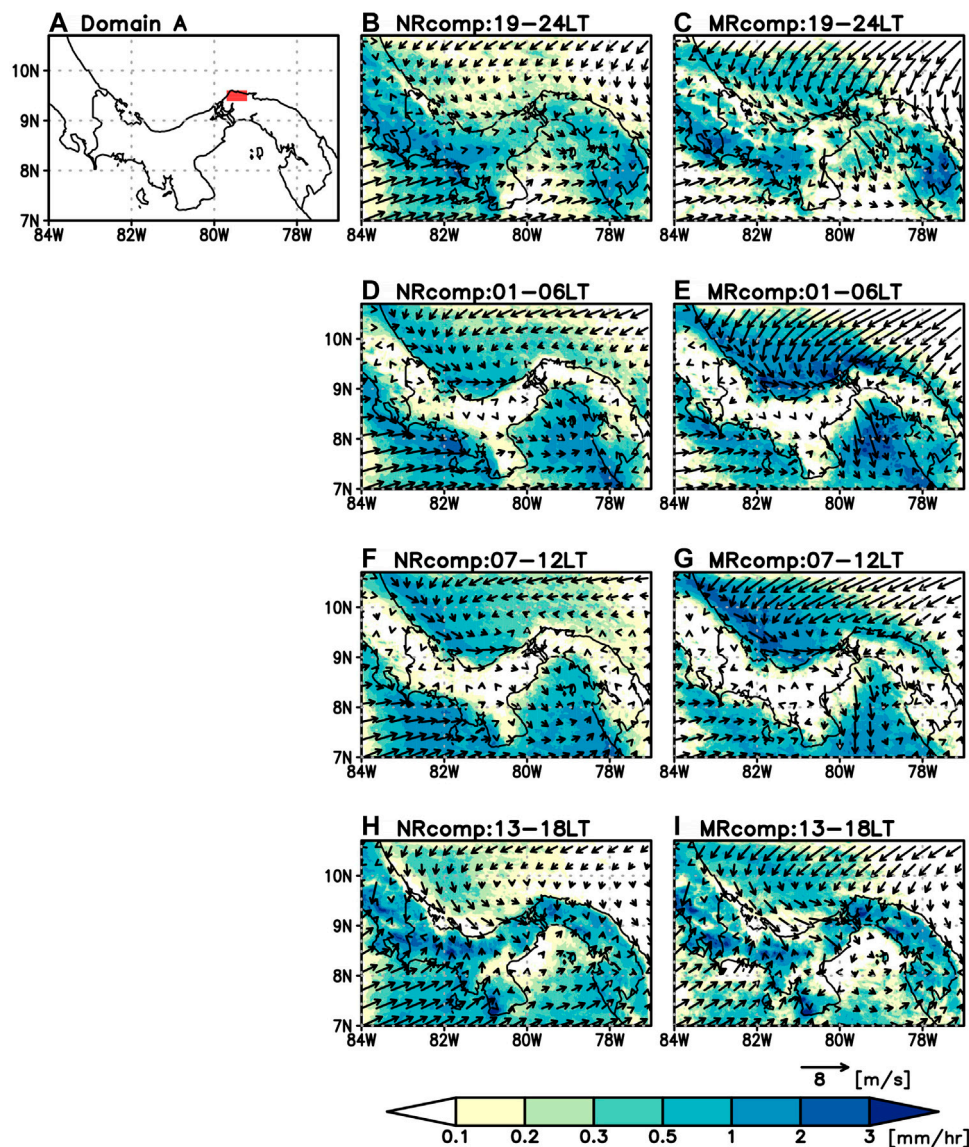


FIGURE 4

Red area indicates domain A (79.2–79.7°W, 9.4–9.6°N), where the morning rain was calculated (A). Composite analysis of the modeled precipitation and surface wind of NHRCM02 for NRcomp [center column; (B, D, F, H)] and MRcomp [right column; (C, E, G, I)].

variation with a maximum at 04–06 LT in the east of the headland of Panama over the Caribbean Sea (Figure 5B). At its peak, this easterly wind extended to the western part of the headland. Westerly winds are dominant in the western Caribbean Sea for the rest of the day, and the westerly extends from the western Caribbean Sea to near the Panama Canal for 14–18 LT. Thus, on this cross section, the prevailing wind direction and its peak are different on the east and west sides of the headland. Northerly winds are enhanced from 18 LT to midnight over the Caribbean Sea, while on land, weak southerly winds prevail around 00–08 LT (Figure 5C). When morning rain occurs, an anomalous easterly was dominant more than 24 h before the occurrence of the morning rain over the Caribbean Sea (Figure 5B, day-1). Anomalous easterly winds extend into 82°W, where the westerly wind normally prevails. The easterly wind anomalies amplified the diurnal change of the

easterly winds as the anomaly was intensified in the morning and weakened in the afternoon. After 18 LT of day-1, the westerly wind anomalies began to strengthen over the western Caribbean Sea. This leads to intensified convergence over land together with amplified easterly winds, which may contribute to the onset of morning rain from midnight to early morning. The anomalous northerly is synchronously intensified with the easterlies more than 24 h prior to the occurrence of morning rain (Figure 5C, day-1).

To confirm the strengthening wind speed from a large-scale view, a composite analysis was performed for the MRI-AGCM3.2, which drove the NHRCMs. Figure 6 shows the vertical profiles of northerly and easterly winds at 80°W. When no morning rain was observed, the axis of the strong easterly wind was located around 15°N, and the westerly wind was blowing at a lower level around Panama (Figure 6A). When morning rain occurs, the strong easterly

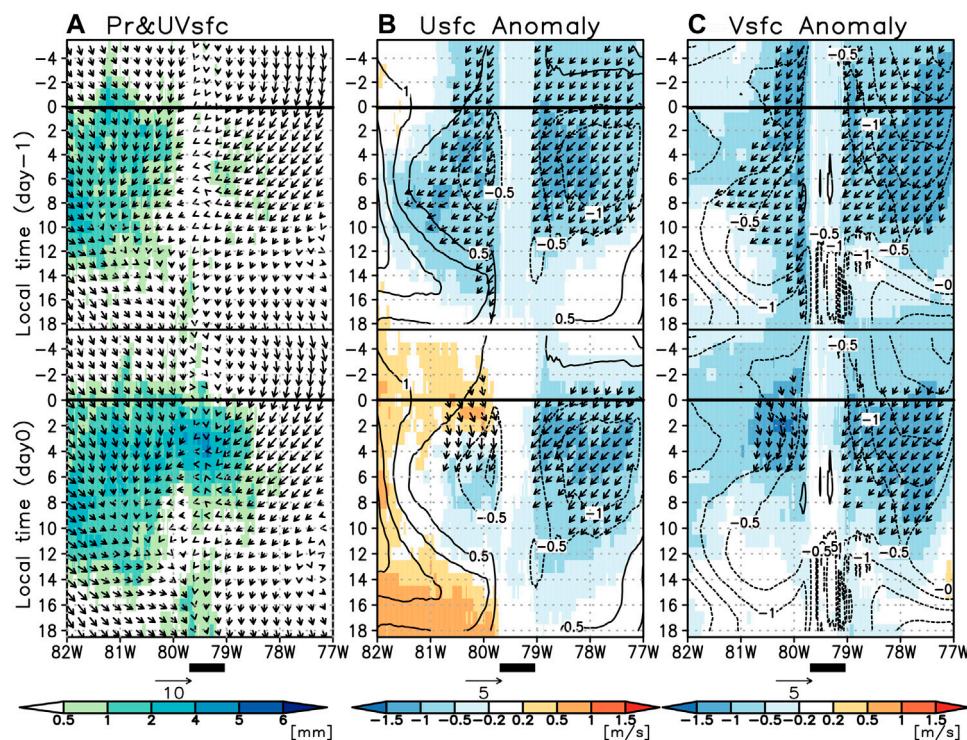


FIGURE 5

Two-day composited precipitation and winds of the longitude–time section at 9.5° N when the morning rain was >1 mm on day0 and <1 mm on day-1. Surface winds (arrows) and precipitation (shading) are shown in (A). Anomalous easterly and northerly wind speeds are denoted by the shading in (B) and (C), which is overlaid on the climatological wind speed indicated by the contours. Arrows in (B) and (C) indicate the anomalous surface winds when the anomalous wind speeds exceed 1 m/s.

winds shift toward Panama (Figure 6B). Intensification was especially remarkable in the lower levels. In addition, northerly winds in the lower levels were also very enhanced north of Panama. Northerly wind speeds exceeded more than twice the speed of those in NRcomp. We analyzed the correlation coefficient of 925 hPa wind speeds with the morning rain over domain A to confirm the spatial extent of the relationship, as shown in Figure 7. The correlation was calculated using daily mean wind speeds and morning rain (7–12 LT) on the corresponding day. Although the morning rain occurred in a small area, the correlation map showed an apparent relationship with lower wind speeds, as expected from the composite analysis in Figure 6. Figure 7 shows a relatively high correlation of easterly winds over the southern Caribbean Sea and the eastern Pacific Ocean. A small relationship was expected with variability of the low-level jet in the Caribbean Sea. A high correlation with northerly winds was found in the southern Caribbean Sea with the center at 80°W, 12.5°N, which is located approximately 300 km away from the headland of Panama. This indicated that low-level northerly wind enhancement in the area leads to atmospheric conditions where the local morning rain occurred over land. To check water vapor transport at the morning rain event, Figure 8 shows the vertically integrated horizontal moisture flux and its convergence. Northeasterly wind anomalies originating from the eastern Caribbean Sea strengthened at 1 LT of day-1 before the morning rain event, and the moisture fluxes converged around Panama. Vertical cross sections at 80°W showed that

strengthening of the northeasterly component was limited to the lower 850 hPa. Descending flows were dominant over the Caribbean Sea, which contributed to the suppression of convection. The northerly component was further enhanced on day0, and the vertically integrated moisture flux flows from the central Caribbean Sea toward the equatorial Pacific Ocean. The northerly wind anomalies thicken into the mid troposphere, and the strong upwelling anomalies that are suggestive of deep convection were found around the north coast of Panama. These results suggest that morning rains occur concurrently with the southwesterly wind enhancement that starts in the lower troposphere and carries water vapor toward the equatorial Pacific with increasing thickness.

4 Discussions

The Caribbean low-level jet (CLLJ) is closely related to precipitation in the Caribbean and North America, as demonstrated by previous studies (Amador, 2008; Cook and Vizy, 2010; Nakaegawa et al., 2014b). However, the correlation coefficient between the daily CLLJ index proposed by Wang (2007) and the amount of morning rain is low (figure not shown). A correlation map also shows a small correlation with the easterly wind in the CLLJ region (70–80°W, 12.5–17.5°N). However, a northerly wind component, which pushes the lower

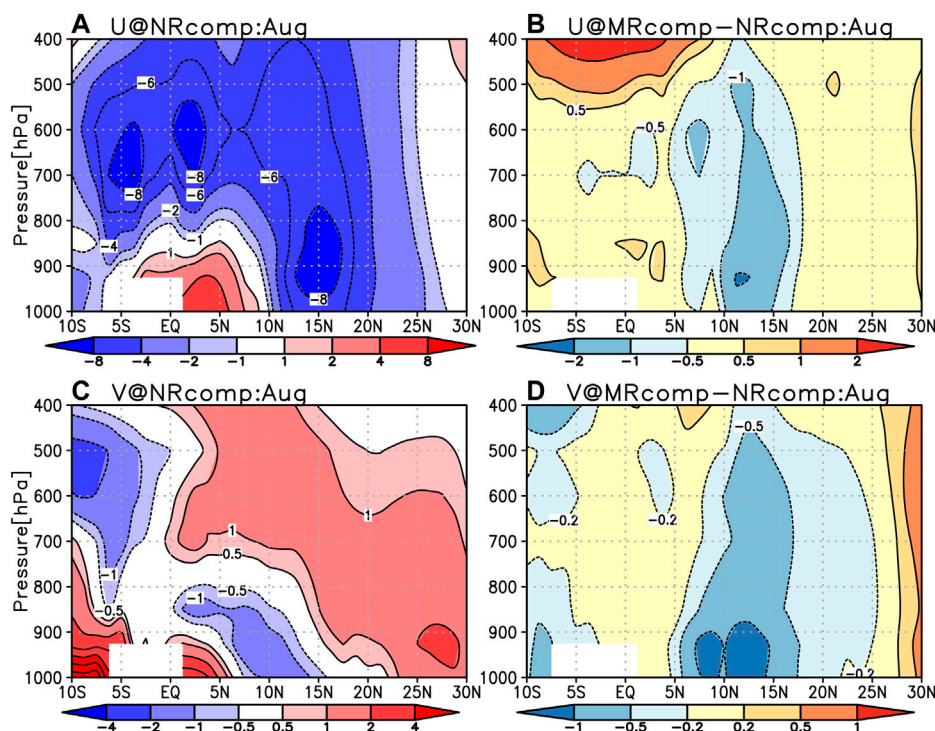


FIGURE 6 Composited vertical section at 80 °W for easterly (A, B) and northerly (C, D) winds in August. The left panels are wind speed in NRcomp, while differences (MRcomp–NRcomp) are shown in the right panels.

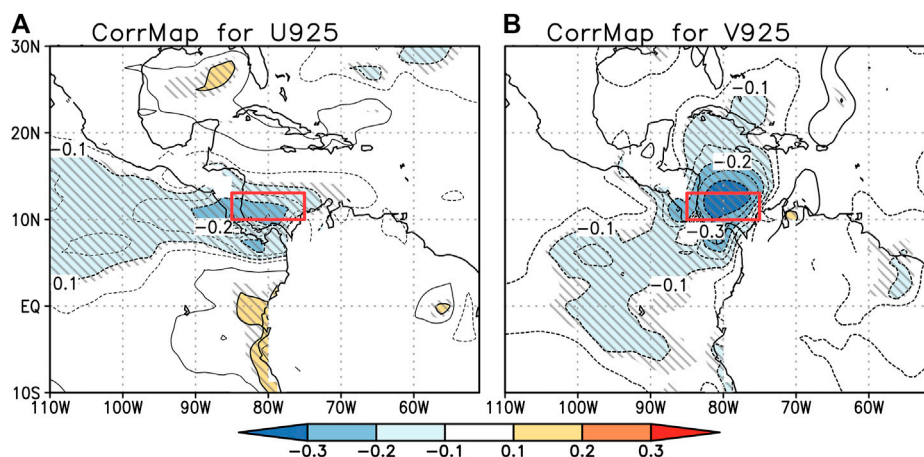


FIGURE 7 Correlation map for easterly (A) and northerly (B) wind speeds at 925 hPa with the amount of morning rain in domain A of Figure 4. Shaded lines indicate ranges that meet the 95% significance level. The red rectangle indicates the area 75–85°W, 10–12.5°N in which the large-scale winds are calculated in Figure 9.

jet down to the south and brings a favorable condition of convergence over the headland, seemed to trigger the morning rain. The westerly wind anomalies over the western Caribbean Sea at midnight one day prior to the morning rain may be associated with enhanced easterly wind anomalies, which blows along the Caribbean coast of Costa Rica and Panama.

Since the land breeze is dominant during the night, the low-level winds effectively converge in the headlands of Panama. The shape of the topography plays an important role. Biasutti et al. (2012) showed that the geometry of the coast and mountain ranges is one of the factors that enhance the local circulation. The headland of northern Panama over the Caribbean Sea is also prone to

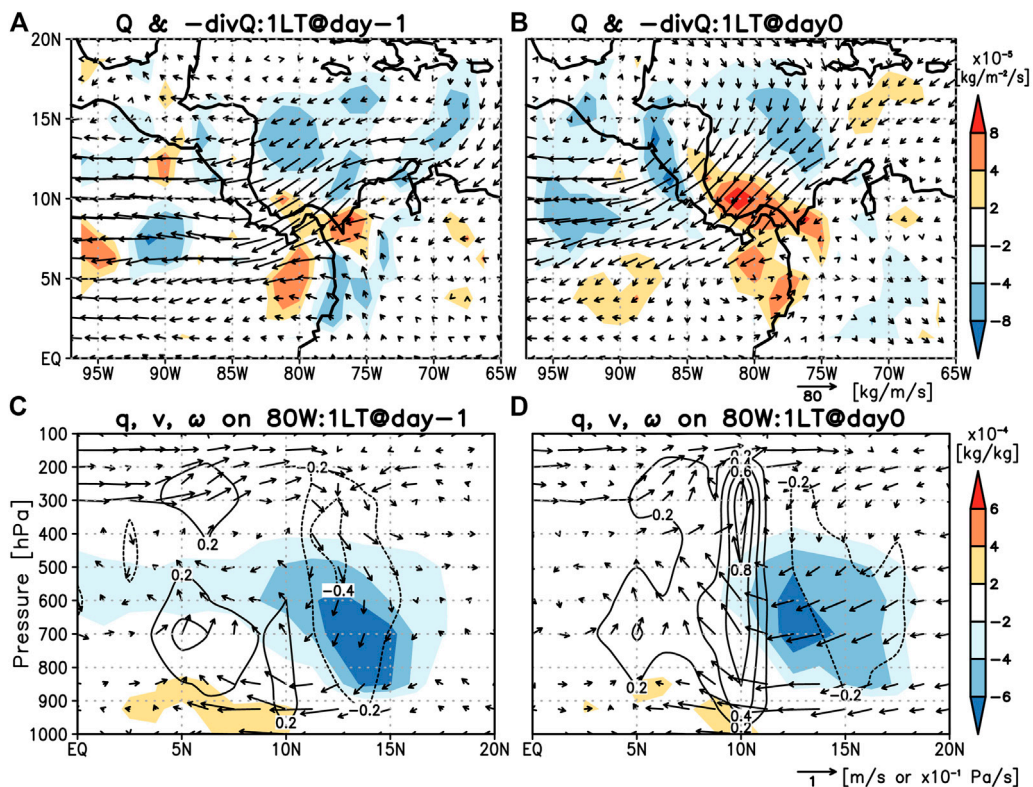


FIGURE 8 Composites vertically integrated moisture fluxes (vectors) and their convergence (shades) at 1 LT on day-1 (A) and day0 (B). A vertical cross section of the meridional and vertical motion of the winds and specific humidity at 80°W on day-1 (C) and day0 (D). The composite was conducted with MRI-AGCM 3.2 and anomalies from the normal state are shown.

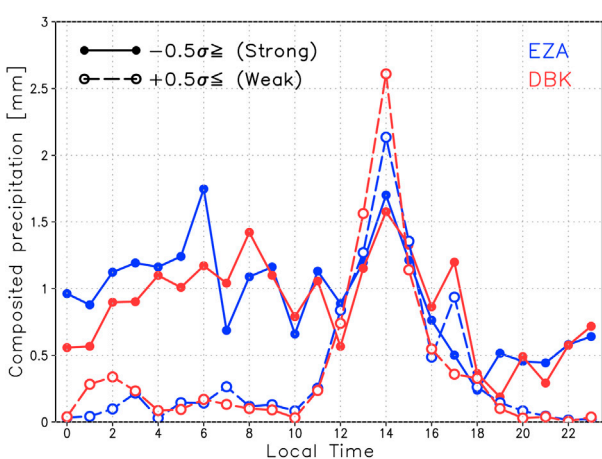


FIGURE 9 Composited precipitation in August at Esperanza (blue) and Dos Bocas (red). The thick solid lines (thick dashed lines) were derived when both the easterly and northerly winds (at 925 hPa) of the JRA-55 reanalysis were relatively strong (weak) over the area 75°–85° W, 10°–12.5° N (red rectangle in Figure 7).

enhanced convection, which is responsible for the occurrence of morning rain. In other words, the local phenomenon of the morning rain is deeply related to large-scale wind change, and it is a

completely different mechanism than the convective activity that occurs over land in the afternoon.

However, these relationships were derived from MRI-AGCM3.2 and dynamically downscaled results. To confirm whether the wind speed variation affects the actual occurrence of morning rain, we examined the relationships using 925 hPa wind speeds from the JRA-55 reanalysis data and the precipitation from rain gauge observations. A composite analysis of precipitation was performed for days when JRA-55 wind anomalies were above and below 0.5 times the standard deviation compared to the mean of each wind component 75–85°W, 10–12.5°N, and were above and below 0.5 times the standard deviation compared to the mean. A red rectangle in Figure 7 indicates the target area. Since the climatological 925 hPa winds in the target area are northeasterly, above average in both components indicates weak northeasterly winds. The period covered was from August in 2000–2016, and the sample size was 204 and 248 days for above and below, respectively. Figure 9 shows the composited rain for EZA and DBK in the northern part of the Upper Chagres River Basin (Figure 1). When the northeasterly wind speeds were relatively strong in the southern Caribbean, the morning rains were noticeable. There was relatively low precipitation with a peak in the afternoon. However, when winds were relatively weak, only afternoon precipitation with a peak at 14 LT was observed with little precipitation at other times of the day. Furthermore, the relationship between the amount of morning rain and the northeasterly was also recognized in other

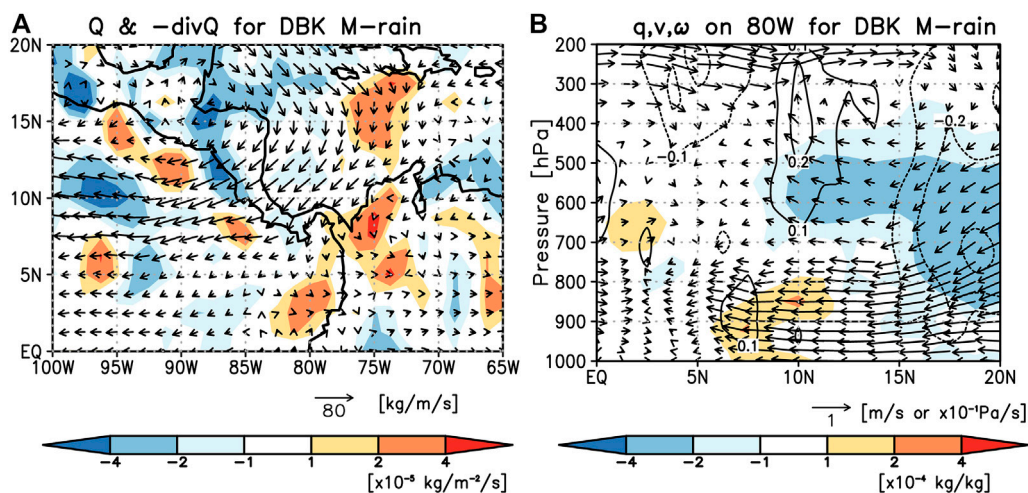


FIGURE 10

Composited vertically integrated moisture fluxes (vectors) and their convergence (shade) at 1 LT on days when the morning rain > 1 mm were observed at DBK in August for the period from 2000 to 2016 (A). A vertical cross section of the meridional motion, vertical motion, and specific humidity at 80°W (B). The composite was conducted with JRA-55 reanalysis, and anomalies from the normal state are shown.

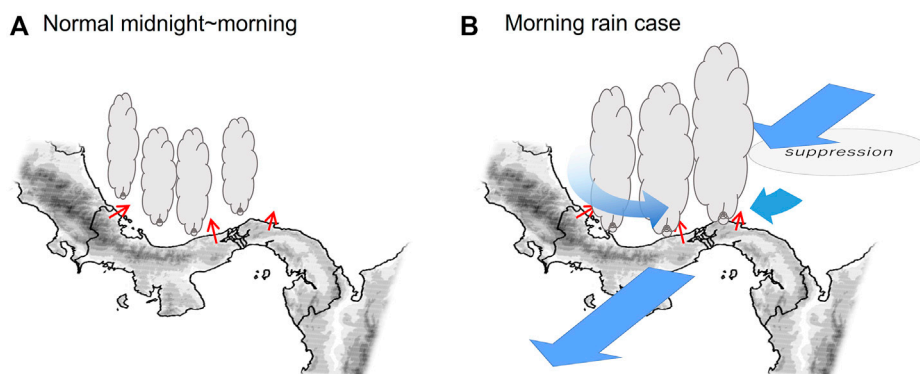


FIGURE 11

Conceptual diagram of the occurrence of morning rains in the north part of the Upper Chagres River Basin. The normal state during the midnight to early morning (A) and the morning rain case (B). Blue (red) vectors indicate anomalous winds (land breeze).

months in the wet season (figure not shown). As confirmed by actual data, it is clear that the local morning rain phenomenon is indeed greatly influenced by the large-scale wind field. Furthermore, we conducted a composite of the reanalysis 3-dimensional fields for days when morning rain was observed at DBK from 2000 to 2016. Although the amplitude of convergence and upwelling motion is lower than the simulated results (Figures 8B,D), a similar pattern of the vertically integrated moisture flux and wind fields was obtained (Figure 10). One possible cause of the weak amplitude is the coarse resolution of the model. Nevertheless, the results support factors that contribute to the occurrence of morning rains, as derived from the simulation data on MRI-AGCM3.2. Based on our analysis, a conceptual diagram of the occurrence of morning rain is shown in Figure 11. Enhanced northeasterly winds in the lower troposphere are accompanied by a descending motion over the Caribbean Sea, which suppresses convection over the ocean at night compared to

the normal state. As the inflow of moisture flux toward the equatorial Pacific further intensifies, the convergence of westerly and easterly wind anomalies near the surface is facilitated with orographic geometry around Panama. As a result and together with the land breeze, deep convection with strong upwelling brings morning rains in the coastal areas of Panama.

This analysis was possible using a high-resolution global model and high-resolution dynamical downscaling experiments as morning rain occurs in a small area. Our findings make it easier to interpret changes in morning rains due to climate change. Nevertheless, NHRCM05 and NHRCM02 revealed some difficulties in representing the peak time of the diurnal cycle and the amount of total precipitation. The smoothed topography and low elevation in NHRCM05 in comparison with NHRCM02 is a possible reason for a low amount of morning rain as the convergence of coastal winds and divergence on mountain slopes is weak in

NHRCM05. The afternoon peak was associated with convective activities caused by land heating during the day. This was generally represented both in NHRCM05 and NHRCM02, but the peak was later than observed regardless of whether or not convective parameterization occurred. Improvements to the boundary layer scheme of the regional climate model would potentially improve this feature. Despite certain challenges, driving the model in various regions and evaluation provides feedback to further advance the model.

5 Conclusion

In this study, factors contributing to morning rain events in the northern part of the Upper Chagres River Basin in Panama were investigated using 5-km and 2-km grid spacing regional climate models nested in a 20-km MRI-AGCM3.2. Enhanced northeasterly winds on the lower troposphere were observed over the Caribbean Sea more than 24 h prior to the morning rain event. An anomalous northeasterly was amplified, especially from the morning to noon, but did not directly lead to the onset of morning rain. Easterly wind anomalies extend into the western Caribbean Sea, where westerly winds are normally dominant, and westerly winds along the coast are enhanced along with nighttime breeze from the land. The nighttime easterly winds were enhanced over northeastern Panama, which resulted in conditions of enhanced convergence over the ocean around the headland of Panama from night to morning. This northeasterly wind anomaly is triggered by enhanced northerly wind anomalies in the southern Caribbean Sea, which pushes the low-level jet southward. Reanalysis data also revealed that strengthening of the low-level winds is related to the occurrence of morning rain. It is clear that the mechanism is quite different from that of thermodynamically generated afternoon precipitation, which is associated with a sea breeze under the landside coastal regime proposed by Kikuchi and Wang. (2008). It is thought that localized morning rains are caused by large-scale wind and topographic effects under the seaside coastal regime. Our findings show that local morning rain events in Panama can be estimated from a large-scale field. Furthermore, the impact on it due to future climate change should be discussed, which is of great importance in assessing the stable future operation of the Panama Canal.

Data availability statement

The data analyzed in this study are subject to the following licenses/restrictions: the data are copyrighted by the Meteorological

Research Institute and an application for use must be submitted. Requests to access these datasets should be directed to ngmn11ts@mri-jma.go.jp.

Author contributions

NI completed the analysis and wrote the manuscript. RP performed the NHRCM05/02 simulations. All authors contributed to the review, discussion, and editing of this article.

Funding

NI, TN, and RP acknowledge the support by JSPS KAKENHI (grant number 20K12154) and the MEXT-Program for the advanced studies of climate change projection (SENTAN) (grant number JPMXD0722680734). NI also acknowledges support by JST (Grant Number JPMJPF2013) and Climate Change Adaptation Research Program in NIES. RP gratefully acknowledges the funding support from SENACYT through the Sistema Nacional de Investigación (SNI-contract 27-2022) and the Centro de Estudios Multidisciplinarios de Ingeniería Ciencias y Tecnología (CEMCIT-AIP), Panamá.

Acknowledgments

The authors would like to acknowledge the constructive comments by reviewers that will improve this manuscript and the corresponding editor.

Conflict of interest

The authors declare that the research was conducted in the absence of any commercial or financial relationships that could be construed as a potential conflict of interest.

Publisher's note

All claims expressed in this article are solely those of the authors and do not necessarily represent those of their affiliated organizations, or those of the publisher, the editors, and the reviewers. Any product that may be evaluated in this article, or claim that may be made by its manufacturer, is not guaranteed or endorsed by the publisher.

References

- Amador, J. (2008). The Intra-Americas sea low level jet: Overview and future research. *Ann. N. Y. Acad. Sci.* 1146, 153–188. doi:10.1196/annals.1446.012
- Biasutti, M., Yuter, S. E., Burleyson, C. D., and Sobel, A. H. (2012). Very high resolution rainfall patterns measured by TRMM precipitation radar: Seasonal and diurnal cycles. *Clim. Dyn.* 39, 239–258. doi:10.1007/s00382-011-1146-6
- Cook, K. H., and Vizy, E. K. (2010). Hydrodynamics of the Caribbean low-level jet and its relationship to precipitation. *J. Clim.* 23, 1477–1494. doi:10.1175/2009JCLI3210.1
- Cruz, F. T., Sasaki, H., and Narisma, G. T. (2016). Assessing the sensitivity of the non-hydrostatic regional climate model to boundary conditions and convective schemes over the Philippines. *J. Meteorological Soc. Jpn.* 94A, 165–179. doi:10.2151/jmsj.2015-059
- Fujita, M., Takahashi, H. G., and Hara, M. (2013). Diurnal cycle of precipitation over the eastern Indian Ocean off Sumatra Island during different phases of Indian Ocean dipole. *Atmos. Sci. Lett.* 14, 153–159. doi:10.1002/asl2.432

- Hirai, M., Sakashita, T., Kitagawa, H., Tsuyuki, T., Hosaka, M., and Oh'izumi, M. (2007). Development and validation of a new land surface model for JMA's operational global model using the CEOP observation dataset. *J. Meteorological Soc. Jpn.* 85A, 1–24. doi:10.2151/jmsj.85A.1
- Houze, R. A., Geotis, S. G., Marks, F. D., and West, A. K. (1981). Winter monsoon convection in the vicinity of North Borneo. Part I: Structure and time variation of the clouds and precipitation. *Mon. Wea. Rev.* 109, 1595–1614. doi:10.1175/1520-0493(1981)109<1595:WMCITV>2.0.CO;2
- Ichikawa, H., and Yasunari, T. (2008). Intraseasonal variability in diurnal rainfall over New Guinea and the surrounding oceans during austral summer. *J. Clim.* 21, 2852–2868. doi:10.1175/2007JCLI1784.1
- Ikawa, M., and Saito, K. (1991). Description of a nonhydrostatic model developed at the Forecast Research Department of the MRI. *Tech. Rep. MRI* 28, 238. doi:10.11483/mritechrepo.28
- Ishizaki, N. N., Takayabu, I., Oh'izumi, M., Sasaki, H., Dairaku, K., Iizuka, S., et al. (2012). Improved performance of simulated Japanese climate with a multi-model ensemble. *J. Meteorological Soc. Jpn.* 90, 235–254. doi:10.2151/jmsj.2012-206
- Kain, J. S., and Fritsch, J. M. (1993). "Convective parameterization for mesoscale models: The Kain-Fritsch scheme," in *The representation of cumulus convection in numerical models*. Editors K. A. Emanuel and D. J. Raymond (Boston, USA: American Meteorological Society), 165–170. doi:10.1007/978-1-935704-13-3_16
- Kawase, H., Murata, A., Yamada, K., Nakaegawa, T., Ito, R., Mizuta, R., et al. (2020). Regional characteristics of future changes in snowfall in Japan under RCP2.6 and RCP8.5 scenarios. *SOLA* 17, 1–7. doi:10.2151/sola.2021-001
- Kieu-Thi, X., Vu-Thanh, H., Nguyen-Minh, T., Le, D., Nguyen-Manh, L., Takayabu, I., et al. (2016). Rainfall and Tropical Cyclone Activity over Vietnam Simulated and Projected by the Non-Hydrostatic Regional Climate Model-NHRCM. *Journal of the Meteorological Society of Japan. Ser. II* 94A, 135–150. doi:10.2151/jmsj.2015-057
- Kikuchi, K., and Wang, B. (2008). Diurnal precipitation regimes in the global tropics. *J. Clim.* 21, 2680–2696. doi:10.1175/2007jcli2051.1
- Kobayashi, S., Ota, Y., Harada, Y., Ebata, A., Mori, M., Onoda, H., et al. (2015). The JRA-55 Reanalysis: General specifications and basic characteristics. *J. Meteor. Soc. Jpn.* 93, 5–48. doi:10.2151/jmsj.2015-001
- Lin, Y. L., Farley, R. D., and Orville, H. D. (1983). Bulk parameterization of the snow field in a cloud model. *J. Climatol. Appl. Meteorology* 22, 1065–1092. doi:10.1175/1520-0450(1983)022<1065:BPOTSF>2.0.CO;2
- Mapes, B. E., Warner, T. T., Xu, M., and Negri, A. J. (2003). Diurnal patterns of rainfall in northwestern South America. Part I: Observations and context. *Mon. Wea. Rev.* 131, 799–812. doi:10.1175/1520-0493(2003)131<0799:DPORIN>2.0.CO;2
- Mizuta, R., Oouhi, K., Yoshimura, H., Noda, A., Katayama, K., Yukimoto, S., et al. (2006). 20-km-Mesh global climate simulations using JMA-GSM Model. *J. Meteorol. Soc. Jpn.* 84, 165–185. doi:10.2151/jmsj.84.165
- Mori, S., Hamada, J. I., Yi, T., Yamanaka, M. D., Okamoto, N., Murata, F., et al. (2004). Diurnal land-sea rainfall peak migration over Sumatra Island, Indonesian Maritime Continent observed by TRMM satellite and intensive rawinsonde soundings. *Mon. Weather Rev.* 132, 2021–2039. doi:10.1175/1520-0493(2004)132<2021:DLRPMO>2.0.CO;2
- Nakaegawa, T., Pinzon, R., Fabrega, J., Cuevas, J. A., De Lima, H. A., Cordoba, E., et al. (2019). Seasonal changes of the diurnal variation of precipitation in the upper Rio Chagres basin, Panamá. *Panamá. PLoS ONE* 14 (12), e0224662. doi:10.1371/journal.pone.0224662
- Nakaegawa, T., Arakawa, O., and Kamiguchi, K. (2015). Investigation of climatological onset and withdrawal of the rainy season in Panama based on a daily gridded precipitation dataset with a high horizontal resolution. *J. Clim.* 28, 2745–2763. doi:10.1175/JCLI-D-14-00243.1
- Nakaegawa, T., Kitoh, A., Ishizaki, Y., Kusunoki, S., and Murakami, H. (2014b). Caribbean low-level jets and accompanying moisture fluxes in a global warming climate projected with CIMP3 multi-model ensemble and fine-mesh atmospheric general circulation models. *Int. J. Climatol.* 34, 964–977. doi:10.1002/joc.3733
- Nakaegawa, T., Kitoh, A., Kusunoki, S., Murakami, H., and Arakawa, O. (2014a). Hydroclimate changes over Central America and the Caribbean in a global warming climate projected with 20-km and 60-km mesh MRI atmospheric general circulation models. *Pap. Meteor. Geophys.* 65, 15–33. doi:10.2467/mripapers.65.15
- Ohsawa, T., Ueda, H., Hayashi, T., and Matsumoto, J. (2001). Diurnal variations of convective activity and rainfall in tropical Asia. *J. Meteorological Soc. Jpn.* 79, 333–352. doi:10.2151/jmsj.79.333
- Pinzón, R., Ishizaki, N. N., Sasaki, H., and Nakaegawa, T. (2021). Panama's current climate replicability in a non-hydrostatic regional climate model nested in an atmospheric general circulation model. *Atmosphere* 12, 1543. doi:10.3390/atmos12121543
- Rapp, A. D., Peterson, A. G., Frauenfeld, O. W., Quiring, S. M., and Roark, E. B. (2014). Climatology of storm characteristics in Costa Rica using the TRMM precipitation radar. *J. Hydromet.* 15, 2615–2633. doi:10.1175/JHM-D-13-0174.1
- Saito, K., Kato, T., Eito, H., and Muroi, C. (2001). Documentation of the meteorological research institute/numerical prediction division unified nonhydrostatic model. *Tech. Rep. Meteorological Res. Inst.* 42, 138. doi:10.11483/mritechrepo.42
- Sasaki, H., Murata, A., Hanafusa, M., Oh'izumi, M., and Kurihara, K. (2011). Reproducibility of present climate in a non-hydrostatic regional climate model nested within an atmosphere general circulation model. *SOLA* 7, 173–176. doi:10.2151/sola.2011-044
- Sorooshian, S., Gao, X., Hsu, K., Maddox, R. A., Hong, Y., Gupta, H. V., et al. (2002). Diurnal Variability of Tropical Rainfall Retrieved from Combined GOES and TRMM Satellite Information. *J. Climate*. 15, 983–1001. doi:10.1175/1520-0442(2002)015<0983:DVOTRR>2.0.CO;2
- Takayabu, I., Ishizaki, N. N., Nakaegawa, T., Sasaki, H., and Wongseree, W. (2021). Potential of representing the diurnal cycle of local-scale precipitation in northeastern Thailand using 5-km and 2-km grid regional climate models. *Hydrological Research Letters* 15, 1–8. doi:10.3178/hrl.15.1
- Wang, C. (2007). Variability of the Caribbean low-level jet and its relations to climate. *Clim. Dyn.* 29, 411–422. doi:10.1007/s00382-007-0243-z
- Warner, T. T., Mapes, B. E., and Xu, M. (2003). Diurnal patterns of rainfall in northwestern South America. Part II: Model simulations. *Mon. Wea. Rev.* 131, 813–829. doi:10.1175/1520-0493(2003)131<0813:DPORIN>2.0.CO;2
- Xie, S. P., Xu, H., Saji, N. H., Wang, Y., and Liu, W. T. (2006). Role of Narrow Mountains in Large-Scale Organization of Asian Monsoon Convection. *J. Climate*. 19, 3420–3429. doi:10.1175/JCLI3777.1
- Yang, G. Y., and Slingo, J. (2001). The Diurnal Cycle in the Tropics. *Mon. Wea. Rev.* 129, 784–801. doi:10.1175/1520-0493(2001)129<0784:TDCITT>2.0.CO;2